Supporting Information for Strong Chemical Bond Hierarchy Leading to Exceptionally High Thermoelectric Figure of Merit in Oxychalcogenide AgBiTeO†

Madhubanti Mukherjee and Abhishek K. Singh*

Materials Research Centre, Indian Institute of Science, Bangalore 560012, India

E-mail: abhishek@iisc.ac.in

ICOHP and Phonon dispersion for different supercell

Nature of bonding in a material depends on the relative strengths of the bonds.

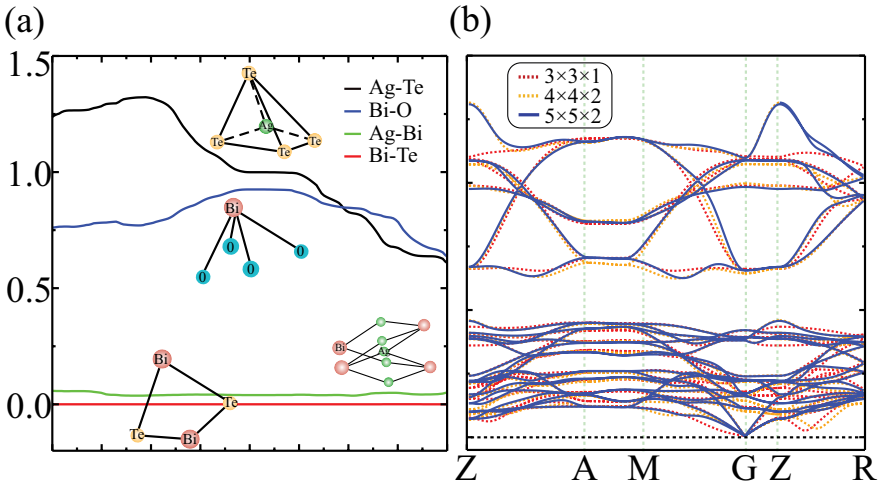

Figure S1: (a) Integrated projected crystal orbital Hamilton population for Ag-Te, Bi-O, Ag-Bi, and Bi-Te bonds with the corresponding structure schematics and (b) phonon dispersions with three different supercell sizes for AgBiTeO.

The integrated projected COHP (IpCOHP) indicates the total bond strength of a chemical bond. We have carried out IpCOHP analysis considering different pair of atoms of AgBiTeO as shown in Figure S1 (a). This shows that nearest neighbor pair of Ag-Te interaction has the largest contribution in integrated COHP, thus confirming the strong bonding between Ag and Te. However, other given pairs involving both Ag and Te show smaller peak in integrated COHP, which confirms that Ag-Te tetrahedra is loosely bonded to the lattice framework.

For $3\times3\times1$, $4\times4\times2$, and $5\times5\times2$ supercell sizes, phonon dispersions in Figure S1 (b) do not show any imaginary phonon spectra, which confirms dynamical stability of AgBiTeO. Well converged supercell of $5\times5\times2$ has been used for all the calculation.

Snapshots of phonon vibrational motions with corresponding Eigen displacements

Vibrational motions for acoustic and low lying optical phonon modes at the Γ point are shown in Figure S2.

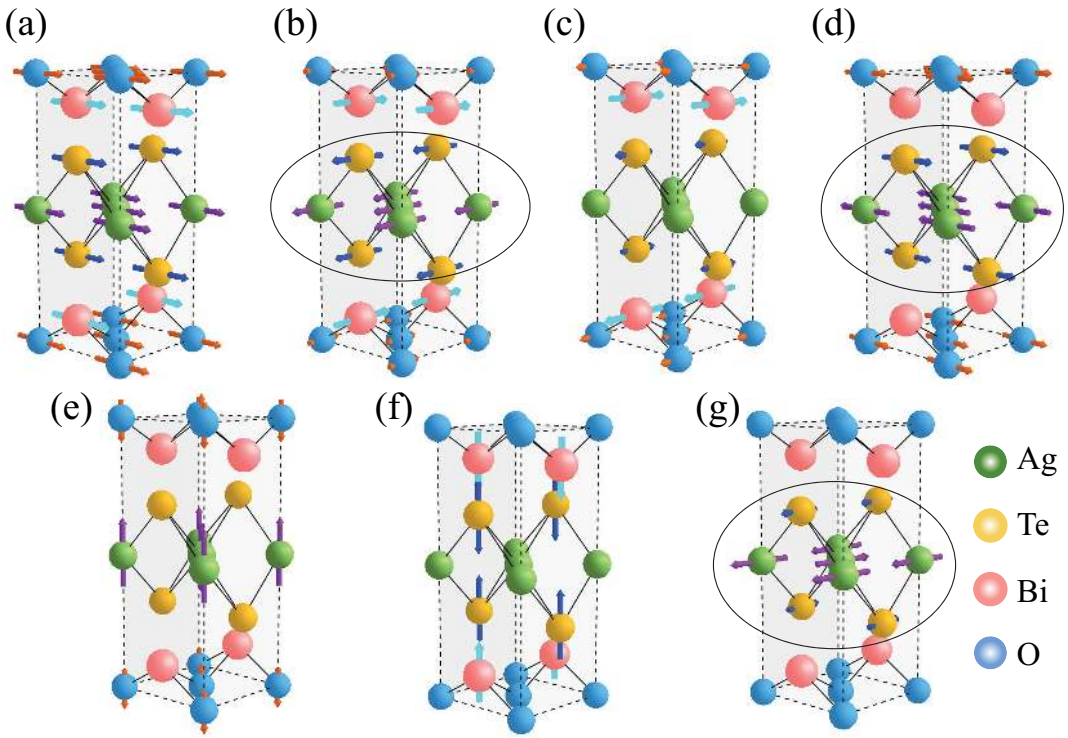

Figure S2: Phonon vibrational modes of (a) longitudinal acoustic and (b)-(g) low lying optical phonon modes.

Large in plane eigen displacements of Ag-Te soft vibrational modes at Γ, as shown in Figure S2 (b), indicates a collective rattling motion. The avoided crossing between phonon modes takes place in between Γ and M, hence, we have considered the vibrations at Γ. Low lying optical phonon mode has a frequency of 1.04 THz, which is close to the avoided crossing frequency of 0.96 THz.

Electronic and thermal transport properties of AgBiSeO

To investigate the hierarchy in AgBiSeO, percentage of ionicity has been calculated. χ_{Ag-Se} between Ag and Se is 0.62, which gives a bond ionicity of 9.1% and χ_{Bi-O} between Bi and O is 1.43 with bond ionicity of 39%. The range of variation in bond strengths thus smaller as compared to AgBiTeO, leading to weaker CBH in AgBiSeO. We also have investigated all the electronic and thermal transport properties in AgBiSeO. Figure S3 (a), (b), and (c) show the calculated Seebeck coefficient, electrical conductivity and powerfactor. Electrical conductivity in AgBiSeO is found to be one order of magnitude smaller as compared to that of AgBiTeO, which results into a smaller powerfactor as well. AgBiSeO also exhibit an ultralow thermal conductivity of 1.04 W/m-K at 300K, as shown in Figure S3 (d).

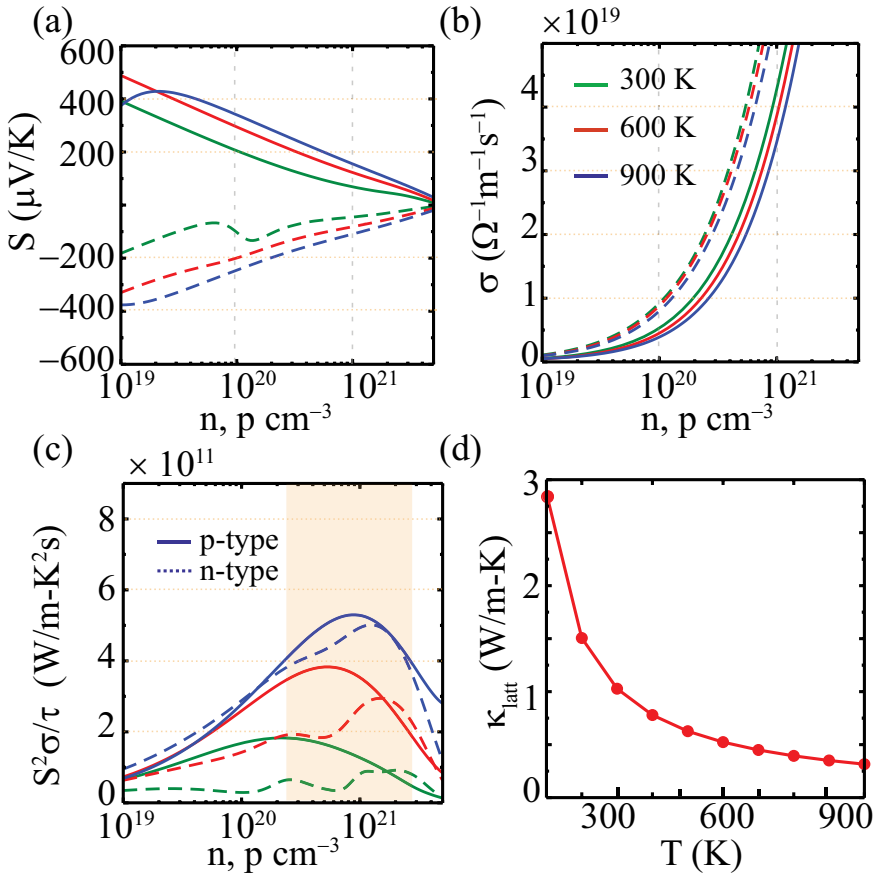

Figure S3: Calculated (a) Seebeck coefficient, (b) electrical conductivity, (c) powerfactor, and (d) lattice thermal conductivity of AgBiSeO.

AgBiSeO is found to be dynamically stable. Calculated phonon lifetime is significantly suppressed, as shown in Figure S4 (a).

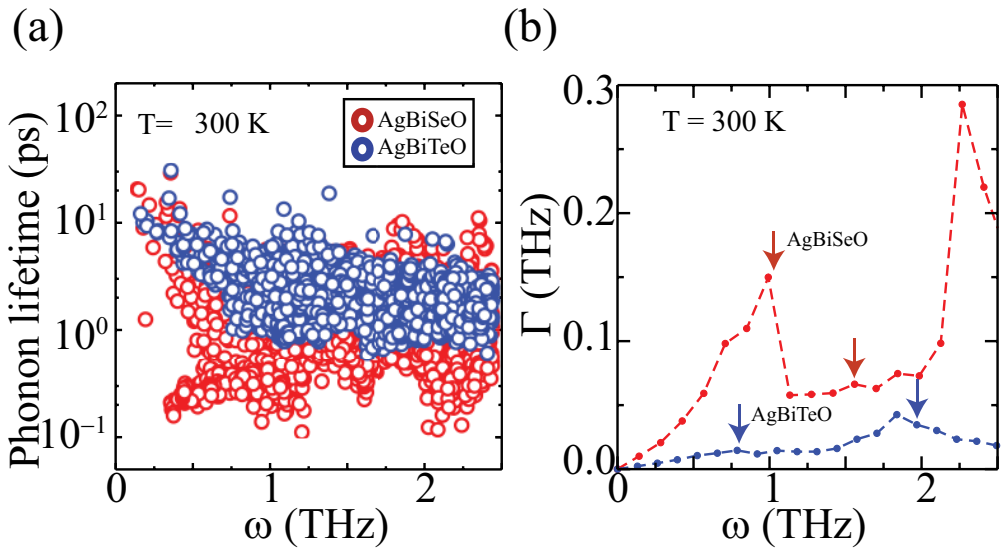

Figure S4: Calculated (a) phonon lifetime and (b) phonon linewidth represented by red and blue curves for AgBiSeO and AgBiTeO, respectively.

The phonon linewidth (Γ), that represents the phonon phonon interaction strength, is shown in Figure S4 (b) for AgBiSeO and AgBiTeO. Larger Γ for AgBiSeO confirms the increased phonon-rattler scattering rate and suggest scattering as the dominant mechanism in AgBiSeO to reduce lattice thermal conductivity.

Temperature dependence of electrical conductivity

The temperature dependence of electrical conductivity, as shown in Figure S5, approximately follow a σ-$T^{-1.4}$ and σ-$T^{-1.24}$ relation for p- and n-type charge carriers, respectively.

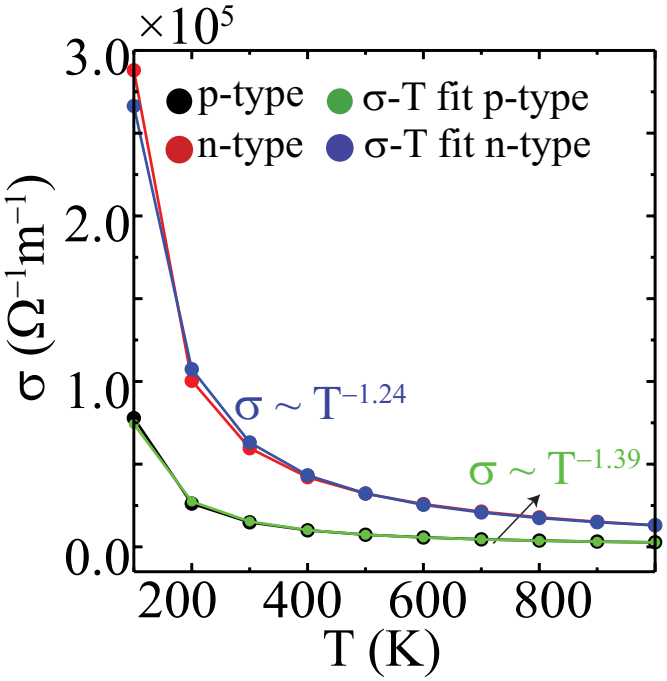

Figure S5: Electrical conductivity of AgBiTeO as a function of temperature after incorporating calculated relaxation time

Figure S5

The temperature exponent of σ-T$^{-1.4}$ for p-type carriers suggests a typical carrier-acoustic phonon scattering,[1] while the temperature exponent -1.24 for n-type carriers indicates a low carrier-phonon scattering.

Electronic relaxation time

The carrier relaxation time (τ) in this work, has been calculated using Bardeen's deformation potential approach.[2] Here, two types of carrier scattering mechanisms have been considered, namely, scattering of electrons with accoustic and optical phonons within the whole operating temperature range of 100-1000 K. The scattering time for electron-accoustic phonon is obtained using the following definition,[3]

$$(\tau(E)_{ac})^{-1} = \frac{(2m^*)^{3/2} D_{ac}^2 k_B T}{2\pi\hbar^4 \rho v_{LA}^2} E^{1/2} \tag{S1}$$

where ρ = ion mass density, m* = effective mass of carriers, and v_{LA} = longitudinal sound velocity, respectively. Deformation potential is denoted by D_{ac} for the aforesaid scattering. To account for the polarity of the compounds, we have estimated the scattering of polar optical phonons with charge carriers, which is obtained by,[3]

$$(\tau(E)_{op})^{-1} = \frac{e^2\omega_{LO}}{4\sqrt{2}\pi\epsilon_0\hbar}\left(\frac{1}{k_\infty}-\frac{1}{k_0}\right)\frac{\sqrt{m^*}}{\sqrt{E}}\Bigg[(n_q+1)$$

$$\times\left(\sqrt{1-\frac{\hbar\omega_{LO}}{E}}+\frac{\hbar\omega_{LO}}{E}\text{sinh}^{-1}\left(\frac{E}{\hbar\omega_{LO}}-1\right)^{1/2}\right)$$

$$+(n_q)\left(\sqrt{1+\frac{\hbar\omega_{LO}}{E}}-\frac{\hbar\omega_{LO}}{E}\text{sinh}^{-1}\left(\frac{E}{\hbar\omega_{LO}}\right)^{1/2}\right)\Bigg]$$

where ω_{LO} = longitudinal optical phonon frequency, k_0 = static dielectric constant , and k_∞ = relative permittivity, respectively. The volume deformation potential for p- and n-type carriers have been determined from the positions of conduction band minima, valence band maxima, and the band gap as a function of applied volumetric strain. Other required parameters such as, relative permittivity and the static dielectric constant are calculated using the Kramers-Kronig relation and Lyddane-Sachs-Teller relation, respectively.[4] As oxychalcogenides are layered structures, thus hold anisotropy of properties. We also calculated the deformation potential for x, y, and z directions by changing the lattice parameters and found that deformation potentials are indeed anisotropic, as given in Table S2. Since the deformation potential constant is anisotropic, the scattering probabilities are expected to be anisotropic too. Hence, we calculated the relaxation time for x, y, and z directions. The scattering probability averaged over x, y, and z directions has been used to calculate the total relaxation time. Figure S6 shows that the order of magnitude of the relaxation time is similar, using volume deformation potential, as well as the directional deformation potential.

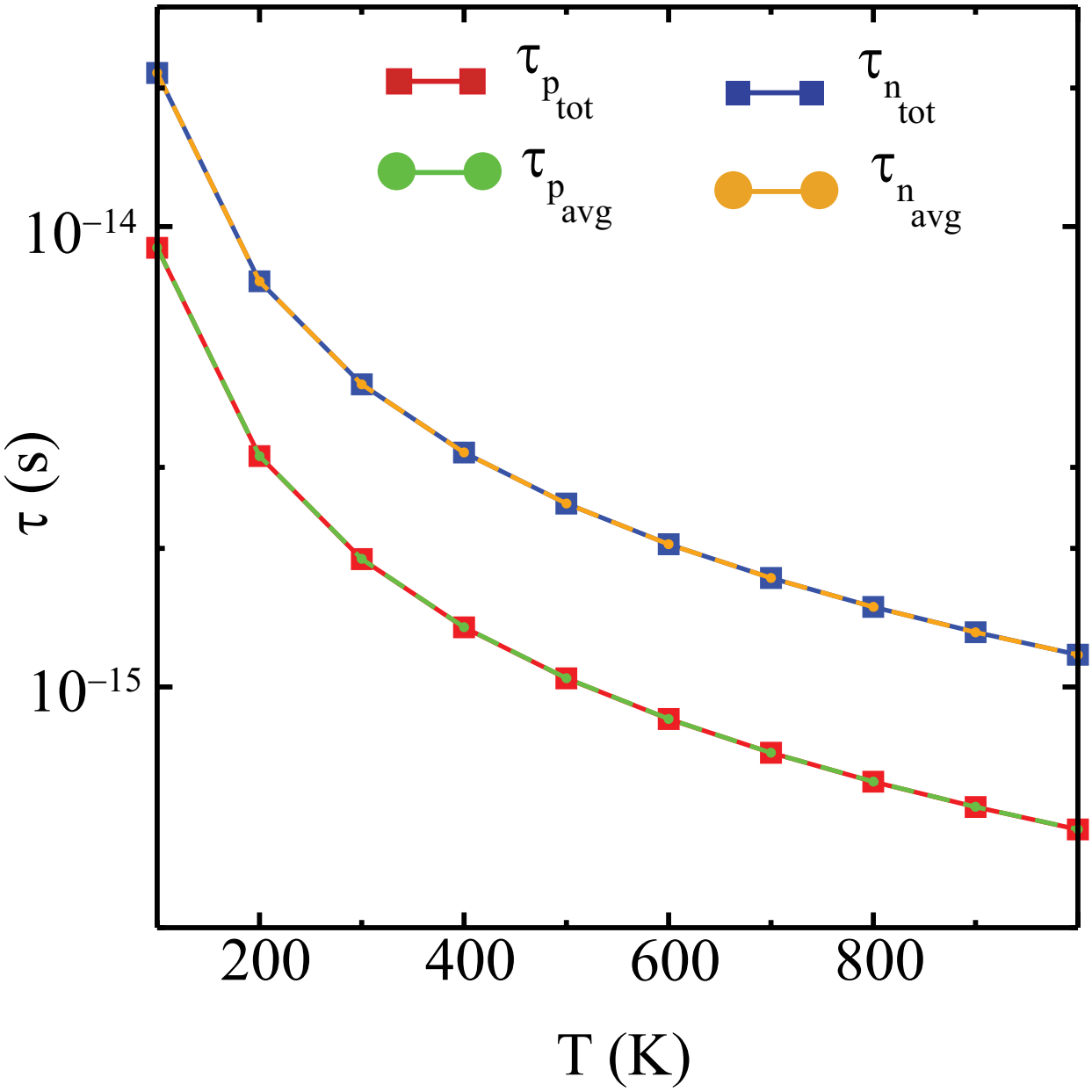

Figure S6: Total and averaged scattering time for p and n type charge carriers

Next, the total carrier relaxation time has been calculated using Mathiessen's rule,

$$\frac{1}{\tau} = \sum_i \frac{1}{\tau_i} \tag{S2}$$

where τ_i is relaxation time for different scattering mechanisms. The quantities and corresponding

values, which have been used to calculate the τ in this work, is given in Table S1.

Table S1: Material parameters used to calculate the electronic relaxation time

Parameter	**symbol**	**value**
Deformation potential for p-type carriers	D_{ac_p}	17.03 eV
Deformation potential for n-type carriers	D_{ac_n}	15.84 eV
Effective mass for p-type carriers	m_p^*	0.57 m_e
Effective mass for n-type carriers	m_n^*	0.10 m_e
Longitudinal sound velocity	$\nu_{g_{LA}}$	3555.44 m/s
Relative permittivity	k_∞	7.72
Static dielectric constant	k_0	13.756
Ion mass density	ρ	9088.69 kg/m^3

Table S2: Deformation potential in x, y, and z directions (eV)

	$\mathbf{D}_x$	$\mathbf{D}_y$	$\mathbf{D}_z$
VBM	16.6	16.6	9.7
CBM	16.6	16.6	9.7

References

(1) Putley, E. H. *The Hall effect and related phenomena*; Butterworth, 1960.

(2) Bardeen, J.; Shockley, W. Deformation Potentials and Mobilities in Non-Polar Crystals. *Phys. Rev.* **1950**, *80*, 72.

(3) Hamaguchi, C.; Hamaguchi, C. *Basic Semiconductor Physics*; Springer, 2001; Vol. 212.

(4) Chang, I. Dielectric Function and the Lyddane-Sachs-Teller Relation for Crystals with Debye Polarization. *Phys. Rev. B* **1976**, *14*, 4318.